Global Biogeochemical Cycles®

RESEARCH ARTICLE
10.1029/2021GB007300

Special Section:
The U.S. GEOTRACES Pacific Meridional Transect (GP15)

Meridional Survey of the Central Pacific Reveals Iodide Accumulation in Equatorial Surface Waters and Benthic Sources in the Abyssal Plain

Rintaro Moriyasu[1], Kenneth M. Bolster[2,3], Dalton S. Hardisty[4], David C. Kadko[5,†], Mark P. Stephens[5], and James W. Moffett[1]

[1]Department of Biological Sciences, University of Southern California, Los Angeles, CA, USA, [2]Department of Earth Sciences, University of Southern California, Los Angeles, CA, USA, [3]School of Ocean Science and Engineering, University of Southern Mississippi, Hattiesburg, MS, USA, [4]Department of Earth and Environmental Sciences, Michigan State University, East Lansing, MI, USA, [5]Applied Research Center, Florida International University, Miami, FL, USA

[†]Deceased

Key Points:

- Iodate is the predominant form of iodine in deep waters, but iodide strongly accumulates in the tropical mixed layer
- Iodide oxidation rates were estimated using complimentary Be-7 data, indicating a half-life in the lower euphotic zone of 3–4 years
- Sediments on the abyssal plain are a modest source of iodide to bottom waters

Supporting Information:

Supporting Information may be found in the online version of this article.

Correspondence to:

J. W. Moffett,
jmoffett@usc.edu

Citation:

Moriyasu, R., Bolster, K. M., Hardisty, D. S., Kadko, D. C., Stephens, M. P., & Moffett, J. W. (2023). Meridional survey of the central Pacific reveals iodide accumulation in equatorial surface waters and benthic sources in the abyssal plain. *Global Biogeochemical Cycles*, *37*, e2021GB007300. https://doi.org/10.1029/2021GB007300

Received 29 DEC 2021
Accepted 20 JAN 2023

Author Contributions:

Conceptualization: Rintaro Moriyasu, James W. Moffett
Data curation: Rintaro Moriyasu, Kenneth M. Bolster, Mark P. Stephens

Abstract The distributions of iodate and iodide were measured along the GEOTRACES GP15 meridional transect at 152°W from the shelf of Alaska to Papeete, Tahiti. The transect included oxygenated waters near the shelf of Alaska, the full water column in the central basin in the North Pacific Basin, the upper water column spanning across seasonally mixed regimes in the north, oligotrophic regimes in the central gyre, and the equatorial upwelling. Iodide concentrations are highest in the permanently stratified tropical mixed layers, which reflect accumulation due to light-dependent biological processes, and decline rapidly below the euphotic zone. Vertical mixing coefficients (K_z), derived from complementary ^{7}Be data, enabled iodide oxidation rates to be estimated at two stations. Iodide half-lives of 3–4 years show the importance of seasonal mixing processes in explaining north-south differences in the transect, and also contribute to the decrease in iodide concentrations with depth below the mixed layer. These estimated half-lives are consistent with a recent global iodine model. No evidence was found for significant inputs of iodine from the Alaskan continental margin, but there is a significant enrichment of iodide in bottom waters overlying deep sea sediments from the interior of the basin.

Plain Language Summary Iodine is an important element in the oceans' biology and chemistry. The two principal forms are iodate and iodide, which were measured on a surface to seafloor survey from Alaska to Tahiti in 2018 as part of the international GEOTRACES program. Iodate, the stable form in the presence of oxygen, was predominant throughout the transect, but iodide was present at the boundaries, including the Alaskan margin, the abyssal plain, and surface waters. A "hot zone" of high iodide comprising up to 50% of the total iodine concentration was detected in tropical surface waters centered on the equator. It reflects accumulation from biological reduction of iodate by phytoplankton coupled with re-oxidation of iodide by a non-light-dependent process. Iodate reduction probably occurs throughout the transect, but winter mixing of surface waters during storms probably smears out this feature in northern waters. This suggests that the turnover between iodide and iodate is longer than seasonal timescales. Indeed, estimates of iodide half-life in the range of 3–4 years were calculated from complimentary shipboard measurements of a short-lived radioisotope, beryllium-7. High iodide in equatorial surface waters is important for atmospheric chemistry as it has a big impact on the global ozone budget.

1. Introduction

Iodine is predominantly found in the inorganic forms of iodate (IO_3^-) and iodide (I^-) in marine environments. It is of biological importance to humans (Hetzel, 1983) and marine microorganisms (Amachi et al., 2007; Farrenkopf et al., 1997; Wong, 2001; Reyes-Umana et al., 2021). Total inorganic iodine, which is defined as the sum of the inorganic forms (Rue et al., 1997), has a uniform distribution in the water column at concentrations ranging between 400 and 500 nM (R. Chance et al., 2014; Luther et al., 1995; Wong et al., 1985) where the oxidized form of IO_3^- is dominant in oxygenated seawater (Wong & Brewer, 1974). However, there are exceptions where the concentrations of I^- are enriched. The highest ocean water column iodide concentrations are found in oxygen-deficient zones (ODZs), where oxygen is absent and respiration is dominated by denitrification. All three of the major ODZs: Arabian Sea (Farrenkopf et al., 1997; Farrenkopf et al., 2002), Eastern Tropic South Pacific (ETSP; G. A. Cutter et al., 2018), and the Eastern Tropic North Pacific (ETNP; Moriyasu et al., 2020) show

Formal analysis: Rintaro Moriyasu, Kenneth M. Bolster, David C. Kadko, Mark P. Stephens
Funding acquisition: James W. Moffett
Investigation: Rintaro Moriyasu, David C. Kadko
Methodology: Rintaro Moriyasu
Project Administration: Rintaro Moriyasu
Resources: Dalton S. Hardisty, David C. Kadko, James W. Moffett
Software: Kenneth M. Bolster
Supervision: James W. Moffett
Validation: Dalton S. Hardisty
Visualization: James W. Moffett
Writing – original draft: Rintaro Moriyasu, James W. Moffett
Writing – review & editing: Rintaro Moriyasu, Dalton S. Hardisty, David C. Kadko, James W. Moffett

high I^- concentrations as a result of the dissimilatory reduction of IO_3^- into I^- (Amachi et al., 2007; Farrenkopf et al., 1997).

The rates of iodate reduction to iodide have been studied in denitrifying systems. Farrenkopf et al. (1997) and Farrenkopf and Luther (2002) reported a rapid reduction of IO_3^- during shipboard incubations in the Arabian Sea. A study on ETNP (Hardisty et al., 2021) found a reduction to occur much more slowly at ≤15 nM/day and in incubation samples taken from depths above the oxycline of the ODZ. These results, along with tracer experiments and model outputs (Babbin et al., 2017), have concluded that IO_3^- is likely to be a terminal electron acceptor in nitrite oxidation (NO_2^-), forming nitrate (NO_3^-), and I^-. Additionally, IO_3^- has also been found to be a terminal electron acceptor for acetate reduction, releasing I^- as a side product (Reyes-Umana et al., 2021).

High concentrations of I^- are also found near the surface (upper 150 m). The origin of surface I^- is thought to be associated with processes that occur during algal growth and, particularly, senescence (Bluhm et al., 2010 Bluhm et al., 2011; Hepach et al., 2020). Surface I^- has been suggested as a tracer for biological activity (R. Chance et al., 2014; Farrenkopf et al., 2002; Luther et al., 1995; Tsunogai & Sase, 1969; Wong et al., 1976). The concentrations of surface I^- vary with latitude; while higher latitudes have between 50 and 100 nM concentrations of surface I^-, lower latitudes can have up to ≥200 nM (Carpenter et al., 2021; R. Chance et al., 2020; Farrenkopf et al., 2002; Nakayama et al., 1989). Biological redox transformations of iodine also lead to the accumulation of organic iodine (Wong & Cheng, 2008), with up to 40 nM concentrations being present in the upper water column in the North Pacific (Huang et al., 2005).

Surface I^- is important for its influence on marine iodine emissions by controlling tropospheric ozone (Sherwen et al., 2016). Such radicals have been proposed to play a key role in the formation of cloud condensation nuclei which can influence the regional climate (Saiz-Lopez et al., 2012). The reaction of I^- and ozone at the sea surface is considered as the dominant source of iodine and a sink for ozone in the atmosphere (MacDonald et al., 2014). Iodine radicals produced in this process participate in other reactions that provide a further sink for ozone and the formation of organo-iodine compounds (Luther et al., 1995). The importance of surface iodide in the atmospheric chemistry of ozone is a major incentive to learn more about what controls its distribution.

While the total iodine concentrations are relatively invariant in the marine water column, they frequently exceed "typical" oceanic values in ODZs. An excess iodine concentration has been previously proposed to be a tracer for O_2 concentration and the redox condition of seawater (G. A. Cutter et al., 2018). In the ETSP and ETNP ODZs, plumes of concentrated I^- up to 1,000 nM—two-fold higher than typical total seawater values—were previously observed. Neither dissimilatory nor abiotic reduction of IO_3^- can explain the magnitude of this plume. The excess iodine diffuses from the reducing shelf sediment into the anoxic waters (G. A. Cutter et al., 2018; Moriyasu et al., 2020) and has also been suggested as a tracer for shelf and margin inputs (G. A. Cutter et al., 2018). Excess inorganic iodine was previously calculated by subtracting the mean total iodine concentration from the measured total inorganic iodine, the sum of IO_3^- and I^- concentrations (Moriyasu et al., 2020). Excess and total inorganic iodine will be referred to, in this work, as excess and total iodine for brevity.

This manuscript explores both the possibility of excess iodine inputs from the oxygenated margin of the Alaskan shelf and the sea surface I^- concentrations along the GEOTRACES GP15 meridional transect. Additionally, using I^- depth profiles from two stations straddling the equator and their corresponding ^7Be data, the rate of I^- oxidation from the mixed layer is estimated. Finally, this manuscript addresses methodological differences in iodide determination through an inter-comparison study.

1.1. Sampling

Samples were taken aboard the R/V *Roger Revelle* (RR1814 and RR1815) along the GEOTRACES GP15 transect along the Pacific Ocean from the shelf of Alaska to Papeete, Tahiti from station 1 (56.1°N, 157.0°W) to station 35 (10.5°S, 152.0°W) between 18 September 2018 and 24 November 2018 (Figure 1). Note that only a subset of all of the GEOTRACES stations and samples were collected for iodine-dictated in part by available freezer space.

The samples were collected using the GEOTRACES trace metal clean carousel equipped with a Seabird CTD, with calibrated sensors for temperature, conductivity, pressure, transmissometer, and oxygen. The chlorophyll fluorescence data were obtained from the shipboard CTD deployed by the Ocean Data Facility (Scripps Institution of Oceanography) using a Wetlabs ECO chlorophyll fluorescence detector. The CTD carousel held 24 General

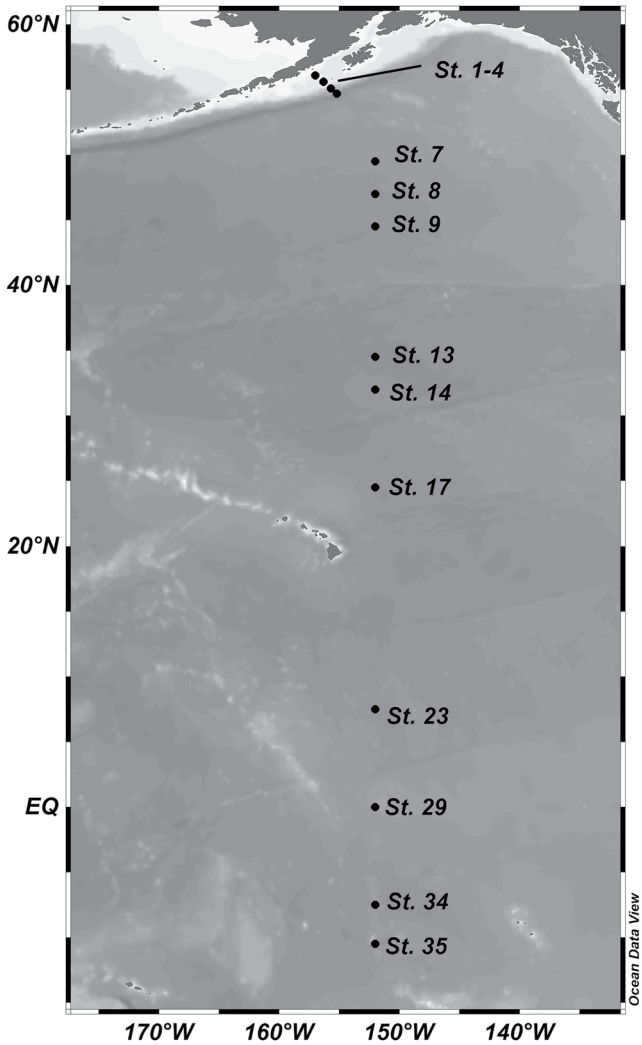

Figure 1. Full transect of GP15. Marked on this map are the locations sampled for iodine speciation.

Oceanics GO-FLO bottles, which were closed at selected depths. Samples were filtered using a 0.2 μm Acropak™ 200 Supor capsule filter (Pall Corporation) and frozen at −20°C. Previous studies on iodine speciation have shown that iodine remains stable over longer periods of time (from months to years) when filtered and frozen (Campos, 1997). Samples were shipped by air in coolers and immediately transferred to −20°C freezers at our laboratory. Each sample was frozen and stored inside a 1 L fluorinated low-density polyethylene (Nalgene; FLPE) bottle. Sample bottles were acid-washed prior to RR1814 and RR1815 cruises following standard trace element and metal acid washing procedures according to the GEOTRACES sampling manual (G. Cutter et al., 2017). While trace element and metal clean procedures were not necessary for the preservation and measurement of iodine speciation, the samples were also collected for trace metal measurements.

1.2. Methods

The electrochemical analyses, for the quantification of I^-, were conducted using the Bioanalytical Systems (BASi) Controlled Growth Mercury Electrode Stand. The Calomel Reference Electrode (BASi; Part #: EF-1352), and the Platinum Wire Auxiliary Electrode (BASi; Part #: MW-1032) were used for analyses. The measurements, for IO_3^- concentrations, used a UV/Vis spectrophotometric method (Perkin Elmer Lambda 35) with a 10 cm quartz cuvette. Measurements were made between wavelengths of 300–500 nm.

1.3. Iodide

Iodide was measured using the Hanging Mercury Drop Electrode (HMDE) with the Cathodic Stripping Square Wave Voltammetry (CSSWV) setting. The method was adapted from Tian and Nicolas (1995) and G. A. Cutter et al. (2018); these workers originally adapted their methods from Luther et al. (1988). The method, used in this work, was further adapted by Moriyasu et al. (2020). The major difference, between the Moriyasu et al. (2020) and the G. A. Cutter et al. (2018) methods, is the inert gas used to purge O_2 from the sample. While G. A. Cutter et al. (2018) used nitrogen (N_2) gas, Moriyasu et al. (2020) and this work additionally opted to use the denser Argon (Ar; Ultra High Purity 99.999%). We noticed differences in measured I^- concentrations between purging with N_2 and Ar. This difference was observed when measuring a crossover station between the GEOTRACES GP15 and GP16 transects at station 35 of GP15 (10.5°S, 152.0°W) (Figure S1 in Supporting Information S1). Both measurements were made with the addition of Sodium Sulfite. We showed that using argon as a purge gas yields better agreement for iodide with an independent mass spectrometric method. Details of this assessment are reported in Supporting Information S1.

The CSSWV method adds a 150 μL aliquot of 0.2% solution of Triton-X 100 (Sigma Aldrich—BioX grade; CAS#: 9036-19-5) to a 10 mL sample prior to being purged under inert Ar gas (Ultra High Purity 99.999%). The samples then required a minimum of 5 min to purge off any remaining O_2 interference. After saying purge, a 50 μL aliquot of 2 M sodium sulfite (Na_2SO_3; Millipore GR ACS; CAS#: 7757-83-7) was added to prevent any remaining O_2 from causing interference, according to the protocol of Tian and Nicolas (1995). The sample was purged for an additional minute and analyzed on the square wave setting. Each sample was measured with a mercury drop size of 6, deposition time of 30 s at −140 mV, and a quiescence time of 5 s. Scan increments were set to 2 mV while the scan range was set between −140 and −700 mV. The amplitude and frequency of the square wave stripping voltammetry were set respectively to 25 mV and 125 Hz and a current range of 1 μA. The height of the peak was calculated at a potential of −300 mV. Standard addition, with potassium iodide (KI; Sigma Aldrich—ACS grade; CAS#: 7681-11-0), was used to determine I^- concentrations in samples and was done in additions of 250 nM to a total of 1,000 nM. The precision of measurement was determined to be ±4 nM (standard deviation with 95% confidence for a sample found to be 243 nM in concentration after five replicates)

in the laboratory (Moriyasu et al., 2020). The limit of detection was 0.34 nM, comparable to the detection of 0.1–0.2 nM reported by Luther et al. (1988), and the limit of quantification was 1.0 nM.

Iodide was determined for samples from the crossover station 35, I^- with Ion Chromatography Inductively Coupled Plasma Mass Spectroscopy (Thermofisher iCAP-TQ) at Michigan State University (Hardisty et al. (2020, 2021) after elution from an AG1-X8 Bio-Rad anion exchange resin. The additions of known I^- concentrations and iodine-free 18.2 m Ω– cm water through the same column procedure was used to assess yields and blanks. Each sample was independently processed in duplicate or triplicate throughout the procedure. The results showed good agreement with the electrochemical method (Table S1 in Supporting Information S1).

1.4. Iodate

Iodate determination was adapted from Rue et al. (1997), who adapted their method from Wong and Brewer (1974). A 1 mL aliquot of 0.12 M sulfanilamide (Sigma Aldrich—ACS grade; CAS#: 63-74-1) in 1% sulfuric acid (Macron Fine Chemicals) was added to a 25 mL sample. The sample was equilibrated with the sulfanilamide solution for 5 min, after which a 1 mL aliquot of a 0.12 M KI (Sigma Aldrich—ACS grade) solution in deionized water was added. The sample was then measured within a minute from the addition of the KI aliquot; the absorbance peak was then measured at 350 nm wavelength. The IO_3^- concentration was determined through standard addition using potassium iodate (KIO_3; Baker Analyzed ™—ACS Reagent; CAS#: 7758-05-6). Precision, based on 5 replicates, was found to be ±12 nM for a seawater sample with 286 nM IO_3^- (Moriyasu et al., 2020). The limit of detection for this method was determined to be ±10 nM and the limit of quantification 30 nM.

2. Results

2.1. Total Inorganic Iodine

Total inorganic iodine was determined as the average inorganic total iodine concentration from the sum of the measured IO_3^- and I^-. Since the region of study were outside any ODZs, all samples were included in our calculation for the mean value since we found very small inputs of margin I^- along the transect. Previously, Moriyasu et al. (2020) found the average concentration to be 475 nM by averaging inorganic iodine measured outside the ODZ (depths ≥1000 m). This average is probably biased highly as a result of residual inputs of excess iodine from within the ODZ and adjacent shelf sediments (Evans et al., 2020). Here, we found that the average total iodine concentration was 430 nM and that total iodine concentrations rarely go above 450 nM in oxygenated waters, except in shelf and surface samples where total iodine exceeded 470 nM on average. Our data, within the central North Pacific, agree with Nakayama et al. (1989), who reported that total iodine concentrations were generally constant at ≤450 nM.

2.2. Iodide and Iodate Along the Main Transect

Iodide concentrations of the top 300 m of the GP15 transect are shown in Figure 2a with the corresponding IO_3^- (Figure 2b), total iodine (Figure 2c), and excess iodine (Figure 2d) concentrations, respectively. Data for each Demi (maximum depth 1,000 m) and Super (full water column) Station are stored at the Biological and Chemical Oceanography Data Management Office (Moriyasu et al., 2022a, 2022b). Most stations along the main transect showed a subsurface I^- maxima. The I^- concentrations were highest at the shallowest samples, which were taken between 20 and 30 m, but there were also increases in I^- concentrations between 50 and 100 m depths. Below 100 m, I^- concentrations dropped to values ≤20 nM, in a range between 2 and 15 nM.

2.3. Iodide in Deep Waters

Iodide values were less than 10 nM in deep waters throughout the transect, except near the seafloor. The results are in good agreement with Nakayama et al. (1989) who reported low values of iodide in deep North Pacific waters (mean value 2.5 nM). However, the values reported by G. A. Cutter et al. (2018) at the crossover station (Figure 3) are at least 100 nM higher. As stated in the Methods Section and Supporting Information, we believe that the difference arises from an interference in G. A. Cutter et al. (2018). Our mixed layer values were significantly higher than those of G. A. Cutter et al. (2018), but this is not surprising given the inherent variability

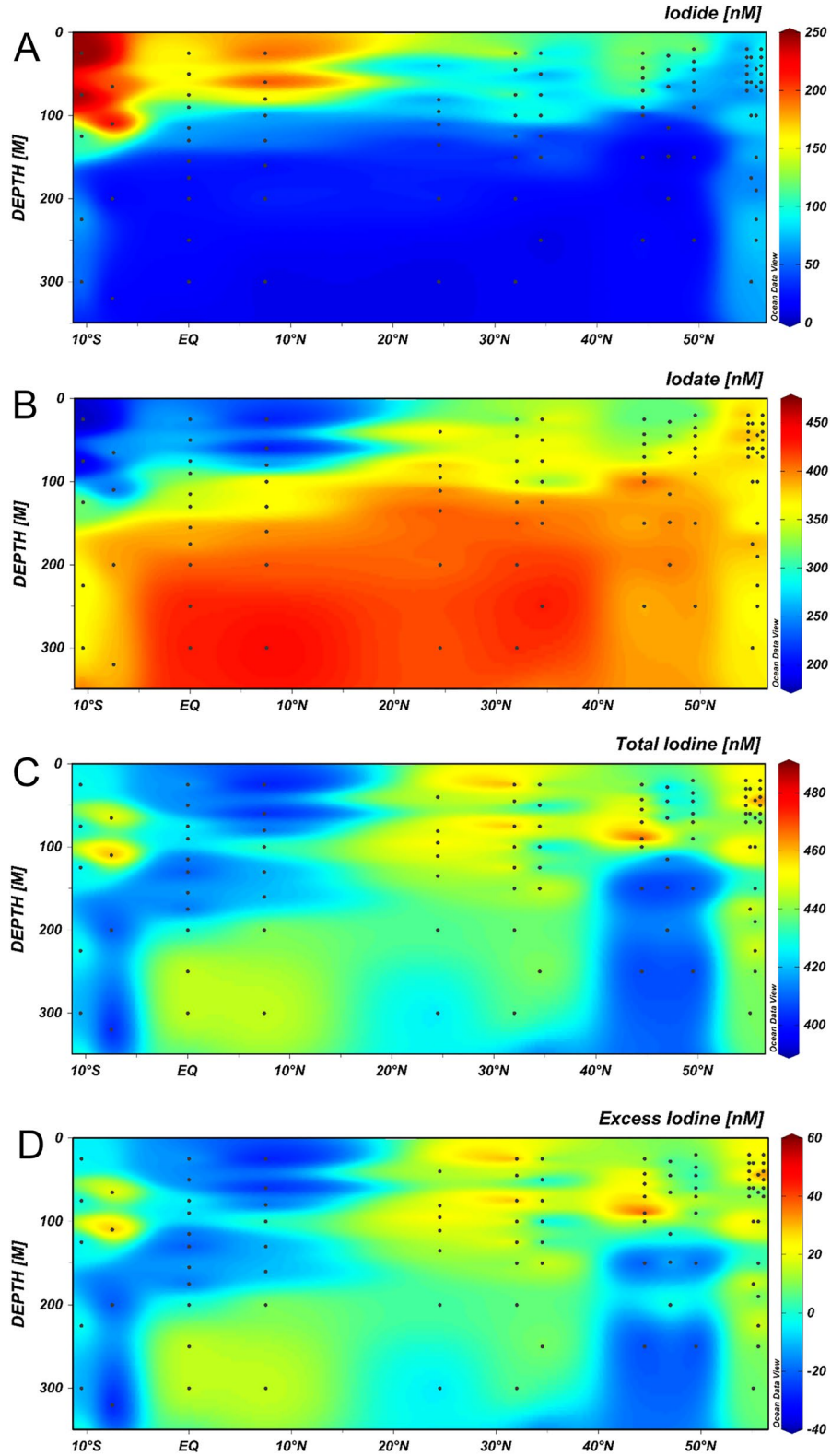

Figure 2. (a–d). The distributions of iodide, iodate, total iodine, and excess iodine along the main GP15 transect from 49.5°N to 10.5°S along the longitude of 152.0°W.

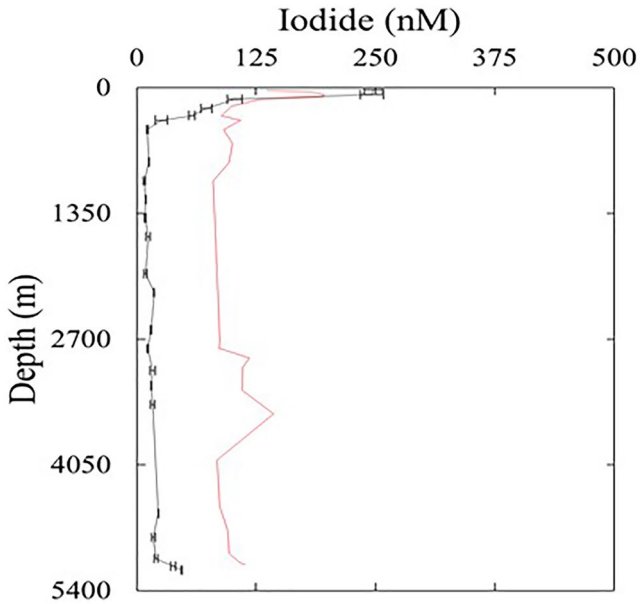

Figure 3. Iodide depth profiles from stations 35 of GP15 and 36 of GP16 (10.5°S, 152°W). Samples, at this station, for GP16 were originally collected in December of 2013, and data reported in Cutter et al. (2018) (red line), while samples for GP15 were collected in November of 2018 (black line).

of water chemistry in the mixed layer and the 5-year time difference between sampling.

We cannot be certain if the low, but detectable values reported by both methodologies in this study and Nakayama et al. (1989) within deep waters (1,000–4,500 m) are real or represent an unresolved interferent at the low nanomolar level. It is not unreasonable for such low values to persist in deep waters where they might arise through lateral advection from margin sources or in situ production within sinking particles.

Bottom water (≥5,000 m) samples were measured for iodine speciation at the super stations (8, 14, 23, 29, and 35). These samples showed a slight elevation of I^- in waters overlying abyssal plain sediments (Figure 4). The elevation is likely to be a result of the benthic release of I^- from the decomposition of organic material at the sediment-water interface (Kennedy & Elderfield, 1987a, 1987b). Iodate remains unchanged, suggesting that the enrichment is "new" iodide and is derived from a benthic source. Nakayama et al. (1989) also reported similar enrichment near the deep North Pacific seafloor, which were particularly prominent in the Japan Trench.

2.4. Iodide Along the Alaskan Shelf

Previous studies focused on the reduced waters on the shelf (G. A. Cutter et al., 2018; Evans et al., 2020; Moriyasu et al., 2020). This study provided information about I^- on the oxygenated shelf of Alaska at stations 1–4

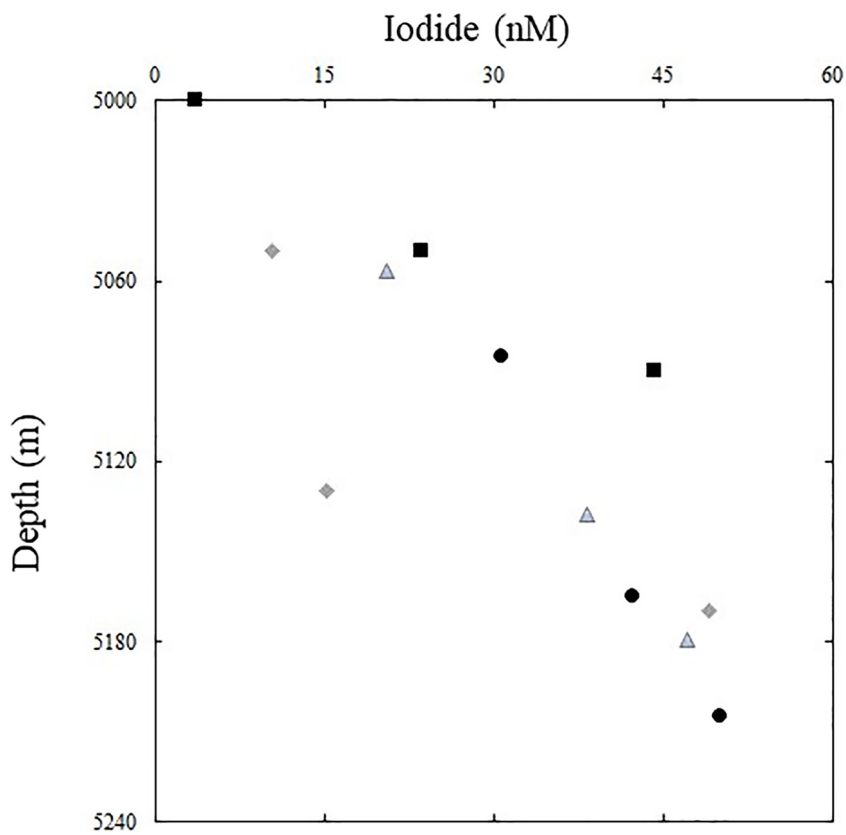

Figure 4. Iodide versus depth near the seafloor at four stations. Station 8 (squares); Station 14 (circles); Station 23 (diamonds); Station 35 (triangles).

Table 1
Rate of Iodide Oxidation, Below the Mixed Layer, Calculated by Forming a 1-Dimensional Model Utilizing ^{7}Be as a Tracer for Vertical Upwelling

Cruise	Station	Lat. (°N)	Long. (°W)	λ (/day)	$t_{1/2}$ (days)
GP15	23	7.5	152.0	4.5 ± 0.3E−04	1,550 ± 90
GP15	35	−10.5	152.0	6.3 ± 0.5E−4	1,100 ± 80
Geometric mean	N/A	N/A	N/A	5.3 ± 0.5E−04	1,300 ± 120

Note. Equations 1 and 2 were fitted to iodide depth profiles at various stations along the GP15 transect to produce the decay constant of surface iodide, λ (/day). The half-life ($t_{1/2}$) was calculated from λ.

(56.1°N, 157.0°W to 54.7°N, 155.0°W). While these stations had observably elevated I^- concentrations, ranging from 50 to 120 nM even at depths as deep as 1,500 m, we did not observe a noticeable plume of excess iodine. By station 4 (54.7°N, 155.0°W), I^- concentrations below the euphotic zone were indistinguishable from the rest of the open ocean water along the main transect (Figure 2a).

2.5. 1-Dimensional Model for the Estimation of Iodide Oxidation

A one-dimensional model was used to estimate the rate of oxidation of iodide below the mixed layer, where there is a well-defined decrease with depth. We utilized beryllium-7 (^{7}Be) data obtained during the cruise to make these estimates. The vertical turbulent diffusion rates (K_z) at two stations, 23 (7.5°N, 152.0°W) and 35 (−10.5°N, 152.0°W), were calculated on the basis of ^{7}Be data (Figure S2 in Supporting Information S1; Kadko, 2020), resulting in 2.0 and 13.0 m^2/d, respectively. Using these K_z values and their corresponding I^- concentrations, we calculated the rate of I^- oxidation at these stations using Equation 1, originally derived in Kadko, (2017):

$$C_{(z)} = C_0 e^{\alpha(z-H)} \quad (1)$$

where C_0 is the constant concentration in the mixed layer, $C_{(z)}$ is the concentration at depth z (in m), and H is the mixed layer depth at the station (44 and 39 m for stations 23 and 35, respectively). The value of α is defined as

$$\alpha = -\sqrt{\frac{\lambda}{K_z}} \quad (2)$$

where K_z is in m^2/day and λ is the decay constant in 1/day. Results can be found in Table 1. Using a non-linear regression on MatLab™, the rate of oxidation (λ), and half-life ($t_{1/2}$) were calculated for these stations (Figure 5).

3. Discussion

3.1. Upper Water Column Iodide and Biological Activity

The highest I^- concentrations throughout the transect were in the mixed layer, reflecting the highest rates of IO_3^- reduction, the lowest rates of I^- oxidation, or both. In general, mixed layer I^- concentrations increased going from high to low latitudes (Figure 2a). Iodide may have more time to accumulate in the permanently stratified tropical stations compared to higher latitudes where seasonal mixing would decrease I^- concentrations through dilution with deeper waters. Our findings are consistent with previous work (R. Chance et al., 2014; R. J. Chance et al., 2019; Nakayama et al., 1989).

The mixed layer inventory of iodide was plotted against net primary productivity (NPP) for all stations (Figure 6). Mixed layer depth and NPP data sources are listed in the SI. Permanently stratified stations have high inventories of iodide (cross symbols in Figure 6), reflecting the enrichment that is clearly visible in Figure 2a, even though NPP is relatively low. Stations further north (circles in Figure 6) show no apparent trend with increasing NPP except at station 3 (far right), near the Alaskan shelf, which has the highest NPP and highest temperate mixed layer iodide inventory. These observations are consistent with our view that seasonal mixing of the more northerly stations constrains how much iodide accumulates in the mixed layer, even when primary production (and hence phytoplankton biomass) is higher further north. The permanently stratified, oligotrophic southern stations enable I^- accumulation at higher levels. Previous compilations have also shown that I^- concentrations are not a simple function of primary production as other factors, such as phytoplankton species composition, temperature, and mixed layer depth, have greater impacts on its distribution (R. Chance et al., 2014).

At most stations along the GP15 transect, subsurface I^- maxima were near the chlorophyll maxima and I^- concentrations tracked the decrease in chlorophyll fluorescence below the chlorophyll maximum (Figure 7). Iodide concentrations plotted against chlorophyll fluorescence at individual stations showed a good correlation (Figure 8). The data are plotted to include and exclude surface samples (above the fluorescence maxima) where data points in red are samples from the fluorescence maxima, and points in black are above the maxima. The

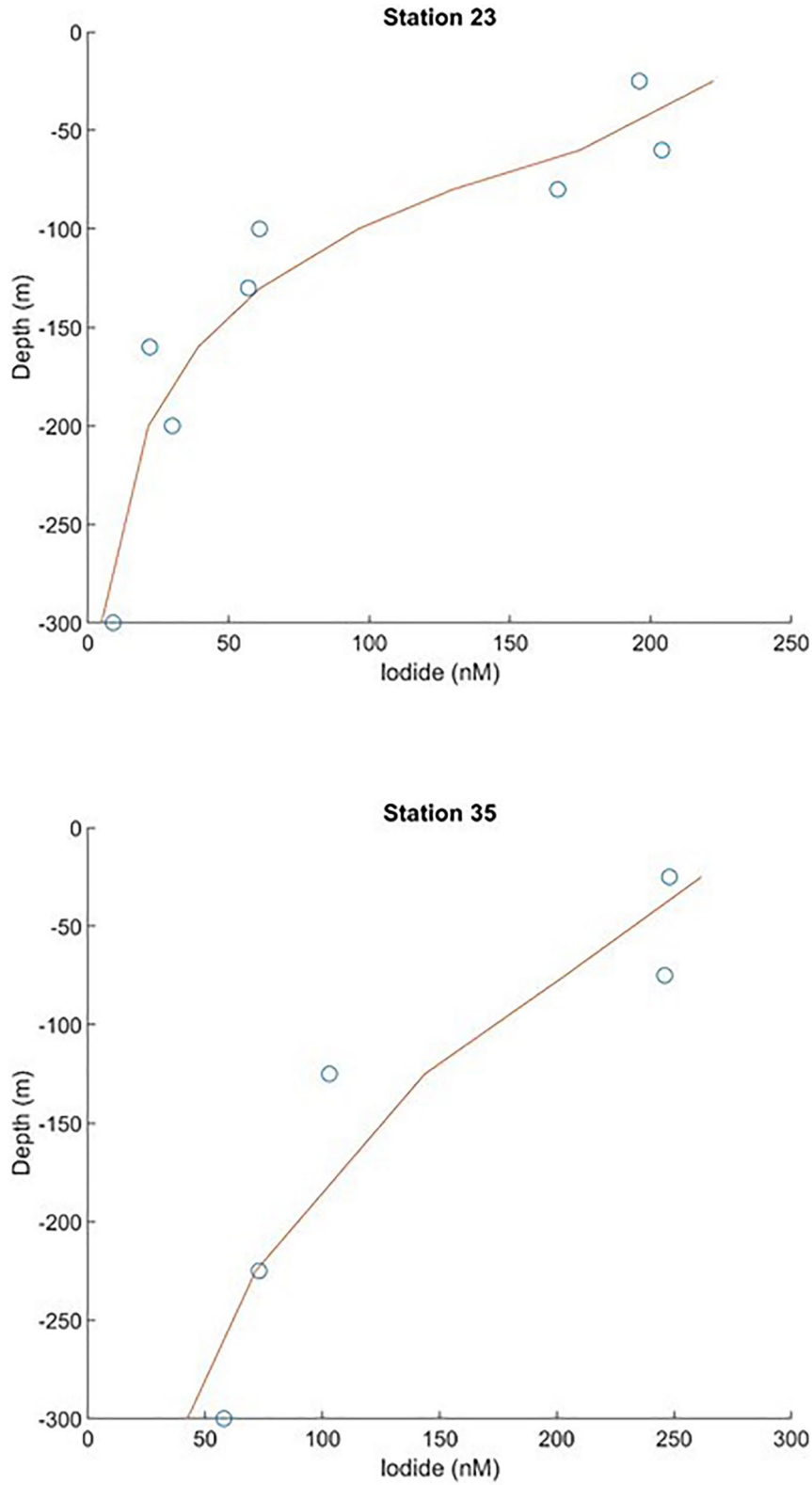

Figure 5. Non-linear regressions (Equation 1: $C_{(z)} = C_{(0)}e^{\alpha(z-H)}$) of Station 23 (7.5°N, 152.0°W) and Station 35 (10.5°S, 152.0°W). The fit was used to calculate the λ, the rate of in situ I^- oxidation below the mixed layer.

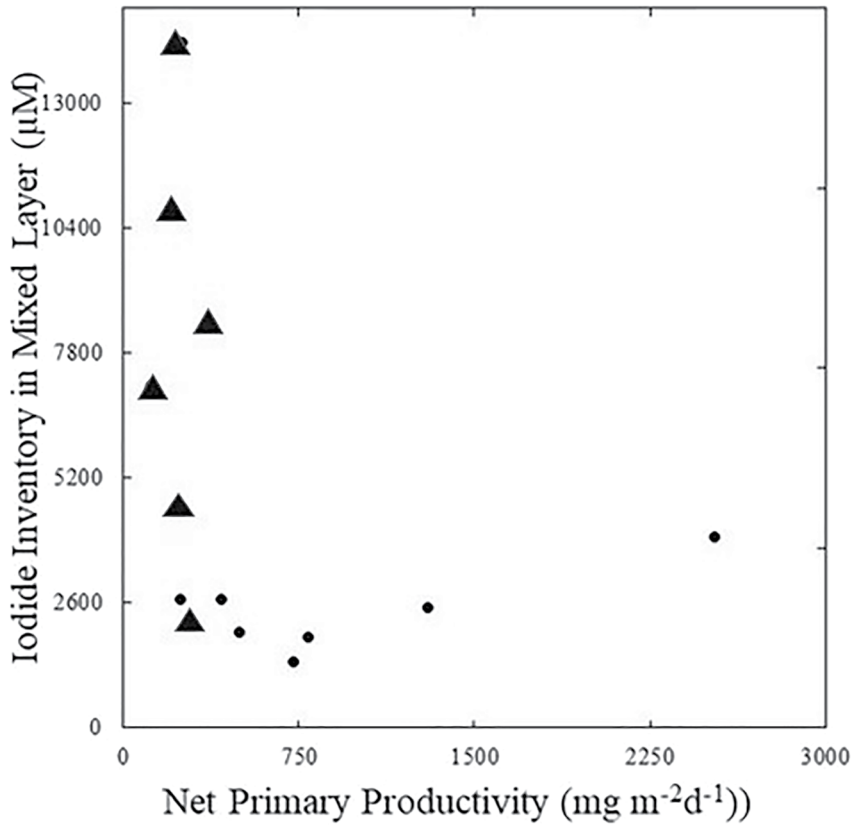

Figure 6. Iodide inventory in the mixed layer versus net primary productivity along the GP15 transect from stations 7–35. NPP was estimated using the MODIS r2018 satellite product and the carbon-based productivity model (Westberry et al., 2008) from Oregon State University Ocean Productivity. Average NPP for 16 days prior to each sampling date was determined using a weighted average of 8-day NPP products within an 18 km by 18 km region containing each station. Data from permanently stratified stations in the south (crosses) and data from seasonally stratified stations in the north (circles).

outlier black points in Figure 8 are above the fluorescence maxima, where the correlation between I^- and fluorescence is poor. High iodide/low chlorophyll in near-surface waters reflected by these data may reflect slow re-oxidation of iodide in the mixed layer rather than elevated production.

The comparison of I^- with fluorescence suggests that IO_3^- reduction by photoautotrophs is a probable source and that the precipitous decline in iodide below the chlorophyll maximum reflects, at least in part, a decrease in production. Phytoplankton have been shown to reduce IO_3^- to I^-, and this may be associated with cell senescence (Bluhm et al., 2010; Hepach et al., 2020). The GP15 cruise did not provide information on phytoplankton physiology or growth rate to determine whether any of the trends we observed could be accounted for by senescence. At stations 13, 14, and 17, local maxima in I^- concentrations coincide with maxima in chlorophyll fluorescence, which may reflect an increase in phytoplankton-derived iodide at those depths.

In their global model of iodide distribution, Wadley et al. (2020) highlighted another important consideration–phytoplankton species composition. Permanently stratified tropical regimes are frequently dominated by the cyanobacteria *Synechococcus* and *Prochlorococcus sp*. *Synechococcus* has high production rates of iodide (Wong et al., 2002), which may contribute to the enrichment we observed.

3.2. Rate of Upper Water Column Iodide Oxidation

Lifetimes for I^- in marine waters have been estimated to be as low as <6 months to up to 40 years (reviewed in R. Chance et al. (2014)). Our work shows that the accumulation of I^- in the permanently stratified tropical mixed layer is more pronounced than in seasonally stratified mixed layers at higher latitudes, suggesting that its redox cycling must be longer than a seasonal time scale. Indeed, results from the 1-D model show that I^- is oxidized

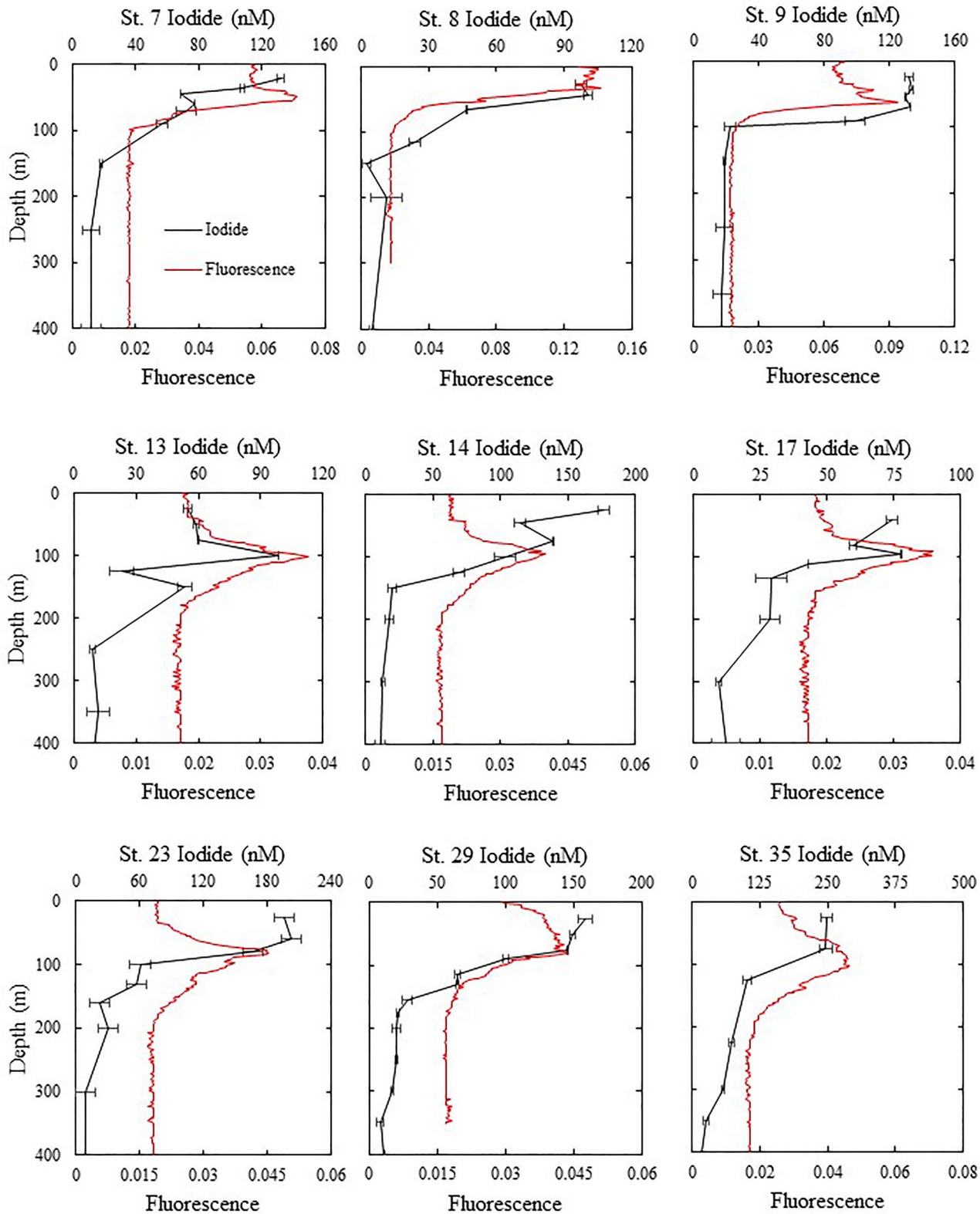

Figure 7. Iodide (black) and chlorophyll fluorescence (red) plotted against depth at Demi and Super Stations in the North Pacific along the GP15 transect (49.5°N, 152.0°W to 0.0°N, 152.0°W). The data plotted correspond to the top 400 m of each station.

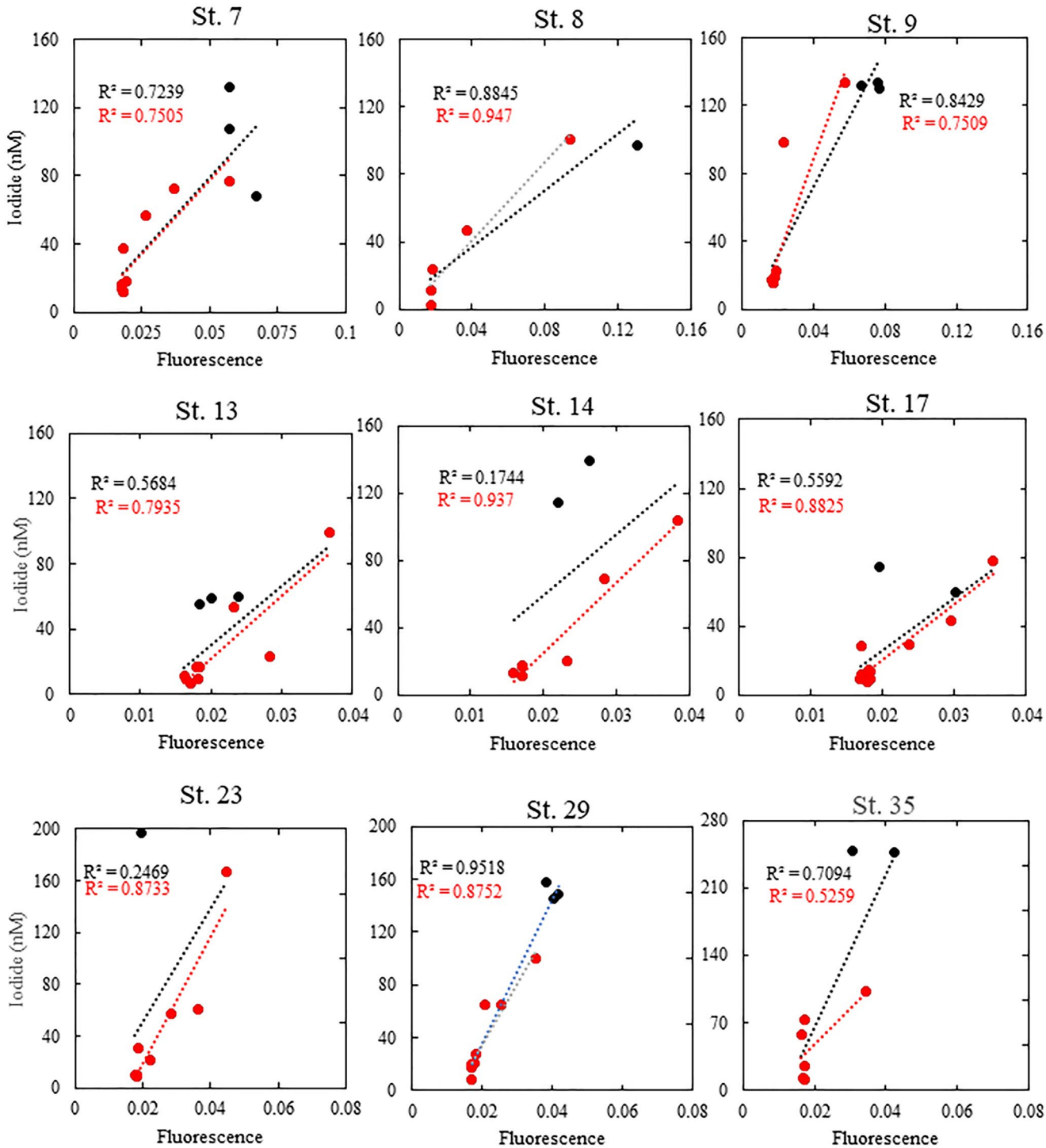

Figure 8. Scatter plots of iodide concentration to chlorophyll fluorescence at individual stations. The black points and line are data which include samples above the fluorescence maxima while the red points and line exclude these data points.

with a half-life between 3 and 4 years (Table 1 modeling). This estimate falls within the range of surface ocean iodide oxidation rates estimated in the model of Wadley et al. (2020) but is above half-life estimates from the global iodide oxidation rate estimated in the cGENIE model (40–50 years; W. Lu et al., 2018). The Wadley et al. (2020) model is dependent on poorly constrained estimates of the iodine:carbon ratio in particulate organic matter and consequently has a rather large range (1–16 years), but our estimates sit squarely within this range. It

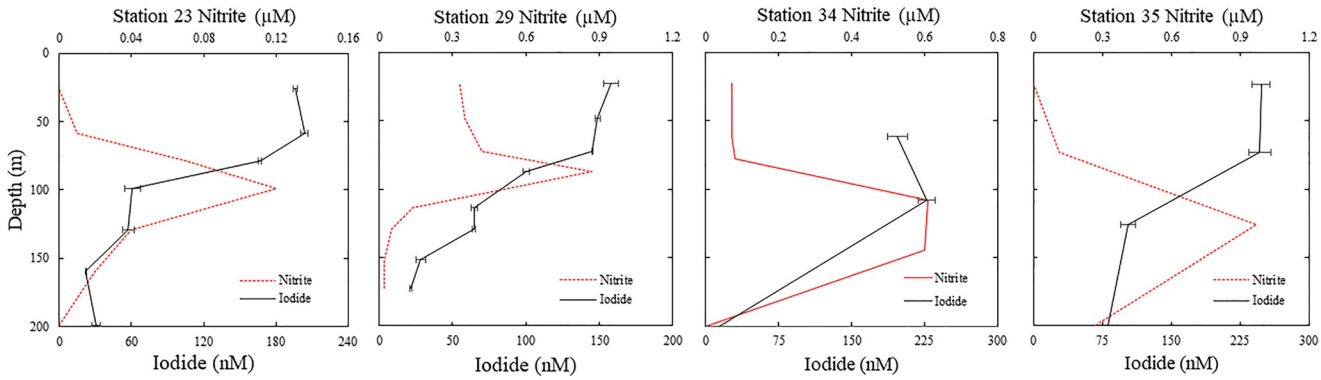

Figure 9. Depth profiles of iodide and nitrite at the four stations near and at the equator were 23 (7.5°N, 152.0°W), 29 (0.0°N, 152.0°W), 34 (−7.5°N, 152.0°W), and 35 (−10.5°N, 152.0°W).

is important to note that our rate estimates are derived by modeling the gradient in iodide below the mixed layer, with the mixed layer concentration in the steady state. The forward oxidation rate of iodide in the mixed layer may be different from our estimate. A scenario where there is rapid turnover of iodate and iodide in the mixed layer cannot be ruled out. It is also possible that the half-life of iodide in the mixed layer may be even longer than 3–4 years. In their global model of iodide distribution, Wadley et al. (2020) found the best fit to the measured distributions when it was assumed that iodide oxidation was correlated with the first step in nitrification: ammonia oxidation. This is consistent with recent data showing that some ammonia oxidizing bacteria can oxidize iodide, while others possess multicopper oxidases (similar to ammonium monooxygenase) that oxidize iodide (Hughes et al., 2021; Long et al., 2015; Truesdale et al., 2001; Yeager et al., 2017). Ammonia oxidation is inhibited at high light intensities and is slow in permanently stratified tropical waters (Horak et al., 2018), so iodide oxidation may also be light inhibited as well. It is also unlikely that there are non-biological oxidative pathways for iodide in the mixed layer (Campos, 1997; Luther et al., 1995).

Iodide drops off sharply at the same depth as the primary nitrite maxima in nearly every station (Figure 9). Primary nitrite maxima are thought to be a zone where ammonium oxidation to NO_2^- occurs at a high rate, slightly exceeding NO_2^- oxidation (the second step in nitrification). The apparent relationship between chlorophyll and iodide (Figures 7 and 8) could reflect the production by phytoplankton, but could equally reflect trends with depth in iodide consumption by bacterial oxidation.

This discussion does not require that iodide oxidation is mediated by ammonium monooxygenase. Iodide-selective pathways have been reported in microbes that are mediated by multi-copper oxidases (Yeager et al., 2017). Other reactions mediated by multi-copper oxidases, (the same family of enzymes that include ammonium mono-oxygenase) such as microbial manganese oxidation (Tebo et al., 2004), are light inhibited (Sunda & Huntsman, 1988).

3.3. Benthic Fluxes as a Source of Iodine to the North Pacific

Previous studies have shown elevated concentrations of excess I^- associated with inputs from the continental shelf. Within ODZs, excess iodine appears to be associated with significant benthic sources associated with highly reducing sediments off of the west coast of India (Farrenkopf and Luther, 2002), Peru (G. A. Cutter et al., 2018), and southern Mexico (Moriyasu et al., 2020). High iodine fluxes under these conditions are consistent with the hypothesis of François (1987), that I^- is displaced by sulfide under reducing conditions and that I^- is released in association with organic matter oxidation, similar to ammonia (Anschutz et al., 2000; Kennedy & Elderfield, 1987a, 1987b). A global model of sulfate reduction rates in sediments suggests that the Alaskan continental margin near the terminus of the GP15 transect is a "hot spot" for sulfate reduction (Bowles et al., 2014). Thus, we anticipated a high concentration of excess iodine in shelf waters, possibly extending as an offshore plume. However, results showed that excess iodine over the Alaskan shelf was less than 40 nM, tenfold lower than the highest values within Pacific ODZs (G. A. Cutter et al., 2018; Moriyasu et al., 2020). While the water above the Alaskan shelf is oxidizing, excess iodine is the sum of I^- and its oxidation product, IO_3^-, and so it should be insensitive to oxidation. It seems more likely that benthic fluxes of iodine from the Alaskan shelf sediments

are simply lower than those in other regimes. At present, we do not have an explanation for this finding. Bluhm et al. (2011) reported a plume of elevated iodide extending north from the Antarctic continent into the South Atlantic but attributed the source to in situ reduction by senescent phytoplankton rather than shelf sediments. One possibility is that benthic fluxes from the Alaskan shelf are high, but the iodine is trapped by organic matter across the sediment-water interface. The organic iodine to total organic carbon (I/TOC) ratios are higher at the sediment-water interface of localities underlying oxygenated water columns relative to those underlying low oxygen water columns (Kennedy & Elderfield, 1987a, 1987b; Z. Lu et al., 2008; Price & Calvert, 1973, 1977; Zhou et al., 2017). This appears to be due to the incorporation of iodine into sedimentary organic matter, which is displaced only by nucleophilic substitution by sulfide. The presence of sulfide in surficial sediments is, of course, highly dependent on the oxygen concentrations in the overlying waters. Given these findings, the elevated concentrations of iodide overlying abyssal plain sediments reported here (Figure 4) might seem surprising, yet they are consistent with high benthic iodide fluxes and significant pore water gradients reported by Kennedy and Elderfield (1987b) in Atlantic deep sea sediments. Sedimentary organic matter is much lower in offshore sediments than in the margins (Chester, 1990; Hesse & Schacht, 2011), so perhaps there is less material to trap iodide at the sediment water interface. This discussion does not answer what is perhaps the most important question of the ultimate source of iodine efflux from sediments. We also do not know where within the interior of the Pacific basin the near-seafloor iodide enrichment comes from. That is because the rates of lateral advection near the seafloor in the North Pacific Basin are typically much higher than the rates of vertical advection (Hautala, 2018), therefore, the iodide measured near the seafloor probably does not come from the immediately underlying sediments.

4. Conclusions

This work synthesizes the distributions of the two main inorganic iodine species along the GEOTRACES GP15 transect and uses complimentary GEOTRACES parameters to estimate the rate of I^- oxidation in the surface oceans. Our results reveal the redox cycling of iodine in the upper water column. Turnover times spanning multiple years contribute to the surface maxima and strong gradients in I^- below the euphotic zone and fall within the range of estimates from a global iodine model. Our estimates were made possible by complimentary ^{7}Be analyses performed on the GEOTRACES GP15 cruise. Permanently stratified, shallow mixed layers in the tropics are associated with high I^- accumulation. We found no evidence for significant inputs of iodine from the atmosphere, Alaskan continental margin, or seafloor. The three major ODZs display the impact of redox cycling on iodine distributions more dramatically. Even in those systems, the ultimate sources of iodine are poorly understood. In particular, continental sources such as major rivers, are understudied.

Conflict of Interest

The authors declare no conflicts of interest relevant to this study.

Data Availability Statement

All data reported here are or will be available in a public repository—the Biological and Chemical Oceanography Data Management Office, available at (https://www.bco-dmo.org/dataset/777951 (Casciotti et al., 2022); https://www.bco-dmo.org/dataset/778168/data; https://www.bco-dmo.org/dataset/873193; https://www.bco-dmo.org/dataset/873183) (Moriyasu & Moffett, 2022a, 2022b); https://www.bco-dmo.org/dataset/781806 (Kadko, 2020).

Acknowledgments
Sampling for this data set was made possible by the scientists and crew participating in the GEOTRACES GP15 cruise. We would also like to thank the crew of the R/V *Roger Revelle* who participated in the RR1814 and RR1815 cruises (the first and second legs of the GP15 transect). Funding for this project was made possible by the National Science Foundation, OCE-1756415, and awarded to James W. Moffett and OCE-1829406 to Dalton Hardisty. We acknowledge Alexi Schnur for analytical assistance. Finally, the International GEOTRACES Program is possible, in part, thanks to the support from the U.S. National Science Foundation to the Scientific Committee on Oceanic Research (SCOR).

References

Amachi, S., Kawaguchi, N., Muramatsu, Y., Tsuchiya, S., Watanabe, Y., Shinoyama, H., et al. (2007). Dissimilatory iodate reduction by marine Pseudomonas sp. strain SCT. *Applied and Environmental Microbiology*, *73*(18), 5725–5730. https://doi.org/10.1128/AEM.00241-07

Anschutz, P., Sundby, B., Lefrancois, L. U. C. I. E., Luther, G. W., III., & Mucci, A. (2000). Interactions between metal oxides and species of nitrogen and iodine in bioturbated marine sediments. *Geochimica et Cosmochimica Acta*, *64*(16), 2751–2763. https://doi.org/10.1016/s0016-7037(00)00400-2

Babbin, A. R., Peters, B. D., Mordy, C. W., Widner, B., Casciotti, K. L., Ward, B. B., et al. (2017). Multiple metabolisms constrain the anaerobic nitrite budget in the eastern tropical south Pacific: Nitrogen dynamics in the eastern tropical south Pacific. *Global Biogeochemical Cycles*, *31*(2), 258–271. https://doi.org/10.1002/2016GB005407

Bluhm, K., Croot, P., Wuttig, K., & Lochte, K. (2010). Transformation of iodate to iodide in marine phytoplankton driven by cell senescence. *Aquatic Biology*, *11*(1), 1–15. https://doi.org/10.3354/ab00284

Bluhm, K., Croot, P. L., Huhn, O., Rohardt, G., Lochte, K., & Rohardt, G. (2011). Distribution of iodide and iodate in the Atlantic sector of the southern ocean during austral summer. *Deep Sea Research Part II: Topical Studies in Oceanography*, *58*(25–26), 2733–2748. https://doi.org/10.1016/j.dsr2.2011.02.002

Bowles, M. W., Mogollón, J. M., Kasten, S., Zabel, M., Hinrichs, K.-U., & Zabel, M. (2014). Global rates of marine sulfate reduction and implications for sub-sea-floor metabolic activities. *Science*, *344*(6186), 889–891. https://doi.org/10.1126/science.1249213

Campos, M. L. A. M. (1997). New approach to evaluating dissolved iodine speciation in natural waters using cathodic stripping voltammetry and a storage study for preserving iodine species. *Marine Chemistry*, *57*(1–2), 107–117. https://doi.org/10.1016/S0304-4203(96)00093-X

Carpenter, L. J., Chance, R. J., Sherwen, T., Adams, T. J., Ball, S. M., Evans, M. J., et al. (2021). Marine iodine emissions in a changing world. *Proceedings of the Royal Society A: Mathematical, Physical & Engineering Sciences*, *477*(2247), 20200824. https://doi.org/10.1098/rspa.2020.0824

Casciotti, K. L., Cutter, K. L., & Lam, P. J. (2022). https://www.bco-dmo.org/dataset/777951

Chance, R., Baker, A. R., Carpenter, L., Jickells, T. D., & Jickells, T. D. (2014). The distribution of iodide at the sea surface. *Environmental Sciences: Processes & Impacts*, *16*(8), 1841–1859. https://doi.org/10.1039/C4EM00139G

Chance, R., Tinel, L., Sarkar, A., Sinha, A. K., Mahajan, A. S., Chacko, R., et al. (2020). Surface inorganic iodine speciation in the Indian and southern oceans from 12°N to 70°S. *Frontiers in Marine Science*, *7*, 621. https://doi.org/10.3389/fmars.2020.00621

Chance, R. J., Tinel, L., Sherwen, T., Baker, A. R., Bell, T., Brindle, J., et al. (2019). Global sea-surface iodide observations, 1967–2018. *Scientific Data*, *6*(1), 286. https://doi.org/10.1038/s41597-019-0288-y

Chester, R. (1990). *Marine geochemistry* (p. 724). Springer.

Cutter, G., Casciotti, K., Croot, P., Geibert, W., Heimbürger, L.-E., Lohan, M., et al. (2017). Sampling and sample-handling protocols for GEOTRACES cruises & appendices (p. 139). https://doi.org/10.25607/OBP-2

Cutter, G. A., Moffett, J. W., Nielsdóttir, M. C., Sanial, V., & Nielsdottir, M. C. (2018). Multiple oxidation state trace elements in suboxic waters off Peru: In situ redox processes and advective/diffusive horizontal transport. *Marine Chemistry*, *201*, 77–89. https://doi.org/10.1016/j.marchem.2018.01.003

Evans, N., Boles, E., Kwiecinski, J. V., Mullen, S., Wolf, M., Devol, A. H., et al. (2020). The role of water masses in shaping the distribution of redox active compounds in the Eastern Tropical North Pacific oxygen deficient zone and influencing low oxygen concentrations in the eastern Pacific Ocean. *Limnology & Oceanography*, *65*(8), 1688–1705. https://doi.org/10.1002/lno.11412

Farrenkopf, A. M., Dollhopf, M. E., Chadhain, S. N., Luther, G. W., Nealson, K. H., & Luther, G. W. (1997). Reduction of iodate in seawater during Arabian Sea shipboard incubations and in laboratory cultures of the marine bacterium Shewanella putrefaciens strain MR-4. *Marine Chemistry*, *57*(3–4), 347–354. https://doi.org/10.1016/S0304-4203(97)00039-X

Farrenkopf, A. M., & Luther, G. W., III. (2002). Iodine chemistry reflects productivity and denitrification in the Arabian Sea: Evidence for flux of dissolved species from sediments of Western India into the OMZ. *Deep Sea Research Part II: Topical Studies in Oceanography*, *49*(12), 2303–2318. https://doi.org/10.1016/S0967-0645(02)00038-3

François, R. (1987). The influence of humic substances on the geochemistry of iodine in nearshore and hemipelagic marine sediments. *Geochimica et Cosmochimica Acta*, *51*(9), 2417–2427. https://doi.org/10.1016/0016-7037(87)90294-8

Hardisty, D. S., Horner, T. J., Evans, N., Moriyasu, R., Babbin, A. R., Wankel, S. D., et al. (2021). Limited iodate reduction in shipboard seawater incubations from the Eastern Tropical North Pacific oxygen deficient zone. *Earth and Planetary Science Letters*, *554*, 116676. https://doi.org/10.1016/j.epsl.2020.116676

Hardisty, D. S., Horner, T. J., Wankel, S. D., Blusztajn, J., Nielsen, S. G., & Blusztajn, J. (2020). Experimental observations of marine iodide oxidation using a novel sparge-interface MC-ICP-MS technique. *Chemical Geology*, *532*, 119360. https://doi.org/10.1016/j.chemgeo.2019.119360

Hautala, S. L. (2018). The abyssal and deep circulation of the Northeast Pacific Basin. *Progress in Oceanography*, *160*, 68–82. https://doi.org/10.1016/j.pocean.2017.11.011.,

Hepach, H., Hughes, C., Hogg, K., Collings, S., Chance, R., & Collings, S. (2020). Senescence as the main driver of iodide release from a diverse range of marine phytoplankton. *Biogeosciences*, *17*(9), 2453–2471. https://doi.org/10.5194/bg-17-2453-2020

Hesse, R., & Schacht, U. (2011). Early diagenesis of deep-sea sediments. *Developments in Sedimentology*, *63*, 557–713. https://doi.org/10.1016/B978-0-444-53000-4.00009-3

Hetzel, B. (1983). Iodine deficiency disorders (IDD) and their eradication. *The Lancet*, *322*(8359), 1126–1129. https://doi.org/10.1016/S0140-6736(83)90636-0.,

Horak, R. E. A., Qin, W., Bertagnolli, A. D., Nelson, A., Heal, K. R., Han, H., et al. (2018). Relative impacts of light, temperature, and reactive oxygen on thaumarchaeal ammonia oxidation in the North Pacific Ocean. *Limnology & Oceanography*, *63*(2), 741–757. https://doi.org/10.1002/lno.10665

Huang, Z., Ito, K., Morita, I., Yokota, K., Fukushi, K., Timerbaev, A. R., et al. (2005). Sensitive monitoring of iodine species in sea water using capillary electrophoresis: Vertical profiles of dissolved iodine in the Pacific ocean. *Journal of Environmental Monitoring*, *7*(8), 804–808. https://doi.org/10.1039/B501398D

Hughes, C., Barton, E., Hepach, H., Chance, R., Pickering, M. D., Hogg, K., et al. (2021). Oxidation of iodide to iodate by cultures of marine ammonia-oxidising bacteria. *Marine Chemistry*, *234*, 104000. https://doi.org/10.1016/j.marchem.2021.104000

Kadko, D. (2017). Upwelling and primary production during the U.S. GEOTRACES east Pacific zonal transect. *Global Biogeochemical Cycles*, *31*(2), 218–232. https://doi.org/10.1002/2016GB005554

Kadko, D. (2020). *Aerosol and seawater beryllium-7 concentrations from leg 2 (Hilo, HI to Papeete, French Polynesia) of the US GEOTRACES Pacific meridional transect (PMT) cruise (GP15, RR1815) on R/V Roger Revelle from October to November 2018*. Biological and Chemical Oceanography data Management Office (BCO-DMO). (Version 1) Version Date 2020-04-20 [if applicable, indicate subset used]. https://doi.org/10.26008/1912/bco-dmo.781806.1

Kennedy, H. A., & Elderfield, H. (1987a). Iodine diagenesis in non-pelagic deep-sea sediments. *Geochimica et Cosmochimica Acta*, *51*(9), 2505–2514. https://doi.org/10.1016/0016-7037(87)90301-2

Kennedy, H. A., & Elderfield, H. (1987b). Iodine diagenesis in pelagic deep-sea sediments. *Geochimica et Cosmochimica Acta*, *51*(9), 2489–2504. https://doi.org/10.1016/0016-7037(87)90300-0

Long, A., Dang, A., Xiao, H., & Yu, X. (2015). The summer distribution of dissolved inorganic iodine along 18°N in the South China Sea. *Journal of Marine Science*, *5*(3). https://doi.org/10.4172/2155-9910.1000169

Lu, W., Ridgwell, A., Thomas, E., Hardisty, D. S., Luo, G., Algeo, T. J., et al. (2018). Late inception of a resiliently oxygenated upper ocean. *Science*, *361*(6398), 174–177. https://doi.org/10.1126/science.aar5372

Lu, Z., Hensen, C., Fehn, U., Wallmann, K., & Wallmann, K. (2008). Halogen and 129I systematics in gas hydrate fields at the northern Cascadia margin (IODP Expedition 311): Insights from numerical modeling. *Geochemistry, Geophysics, Geosystems*, *9*(10). https://doi.org/10.1029/2008GC002156

Luther, G. W., SwartzBranson, C., & Ullman, W. J. (1988). Direct determination of iodide in seawater by cathodic stripping square wave voltammetry. *Analytical Chemistry*, *60*(17), 1721–1724. https://doi.org/10.1021/ac00168a017

Luther, G. W., Wu, J., & Cullen, J. B. (1995). Redox chemistry of iodine in seawater: Frontier molecular orbital theory considerations. In C. P. Huang, C. R. O'Melia, & J. J. Morgan (Eds.), *Aquatic chemistry* (Vol. 244, pp. 135–155). American Chemical Society. https://doi.org/10.1021/ba-1995-0244.ch006

MacDonald, S. M., Gómez Martín, J. C., Chance, R., Warriner, S., Saiz-Lopez, A., Carpenter, L. J., et al. (2014). A laboratory characterisation of inorganic iodine emissions from the sea surface: Dependence on oceanic variables and parameterisation for global modeling. *Atmospheric Chemistry and Physics*, *14*(11), 5841–5852. https://doi.org/10.5194/acp-14-5841-2014.,

Moriyasu, R., Evans, N., Bolster, K. M., Hardisty, D. S., & Moffett, J. W., (2020). The distribution and redox speciation of iodine in the eastern tropical North Pacific Ocean. *Global Biogeochemical Cycles*, *34*(2). https://doi.org/10.1029/2019GB006302

Moriyasu, R., & Moffett, J. W. (2022a). *Inorganic iodine concentrations from leg 1 (Seattle, WA to Hilo, HI) of the US GEOTRACES Pacific meridional transect (PMT) cruise (GP15, RR1814) on R/V Roger Revelle from September to October 2018*. Biological and Chemical Oceanography data Management Office (BCO-DMO). (Version 1) Version Date 2022-04-20. https://doi.org/10.26008/1912/bco-dmo.873183.1.,

Moriyasu, R., & Moffett, J. W. (2022b). *Inorganic iodine concentrations from leg 2 (Hilo, HI to Papeete, French Polynesia) of the US GEOTRACES PMT cruise (GP15, RR1815) on R/V Roger Revelle from Oct-Nov 2018*. Biological and Chemical Oceanography data Management Office (BCO-DMO). (Version 1) Version Date 2022-04-22. https://doi.org/10.26008/1912/bco-dmo.873193.1

Nakayama, E., Kimoto, T., Isshiki, K., Sohrin, Y., Okazaki, S., & Sohrin, Y. (1989). Determination and distribution of iodide- and total-iodine in the North Pacific Ocean - By using a new automated electrochemical method. *Marine Chemistry*, *27*(1–2), 105–116. https://doi.org/10.1016/0304-4203(89)90030-3

Price, N. B., & Calvert, S. E. (1973). The geochemistry of iodine in oxidised and reduced recent marine sediments. *Geochimica et Cosmochimica Acta*, *37*(9), 2149–2158. https://doi.org/10.1016/0016-7037(73)90013-6

Price, N. B., & Calvert, S. E. (1977). The contrasting geochemical behaviours of iodine and bromine in recent sediments from the Namibian shelf. *Geochimica et Cosmochimica Acta*, *41*(12), 1769–1775. https://doi.org/10.1016/0016-7037(77)90209-5

Reyes-Umana, V., Henning, Z., Lee, K., Barnum, T. P., Coates, J. D., & Barnum, T. P. (2021). Genetic and phylogenetic analysis of dissimilatory iodate-reducing bacteria identifies potential niches across the world's oceans. *The ISME Journal*, *16*(1), 38–49. https://doi.org/10.1038/s41396-021-01034-5

Rue, E. L., Smith, G. J., Cutter, G. A., Bruland, K. W., & Bruland, K. W. (1997). The response of trace element redox couples to suboxic conditions in the water column. *Deep Sea Research Part I: Oceanographic Research Papers*, *44*(1), 113–134. https://doi.org/10.1016/S0967-0637(96)00088-X.,

Saiz-Lopez, A., Plane, J. M. C., Baker, A. R., Carpenter, L. J., von Glasow, R., Gómez Martín, J. C., et al. (2012). Atmospheric chemistry of iodine. *Chemical Reviews*, *112*(3), 1773–1804. https://doi.org/10.1021/cr200029u.,

Sherwen, T., Schmidt, J. A., Evans, M. J., Carpenter, L. J., Großmann, K., Eastham, S. D., et al. (2016). Global impacts of tropospheric halogens (Cl, Br, I) on oxidants and composition in GEOS-Chem. *Atmospheric Chemistry and Physics*, *16*(18), 12239–12271. https://doi.org/10.5194/acp-16-12239-2016

Sunda, W. G., & Huntsman, S. A. (1988). Effect of sunlight on redox cycles of manganese in the southwestern Sargasso Sea. *Deep Sea Research Part A: Oceanographic Research Papers*, *35*(8), 1297–1317. https://doi.org/10.1016/0198-0149(88)90084-2

Tebo, B. M., Bargar, J. R., Clement, B. G., Dick, G. J., Murray, K. J., Parker, D., et al. (2004). Biogenic manganese oxides: Properties and mechanisms of formation. *Annual Review of Earth and Planetary Sciences*, *32*(1), 287–328. https://doi.org/10.1146/annurev.earth.32.101802.120213

Tian, R. C., & Nicolas, E. (1995). Iodine speciation in the northwestern Mediterranean Sea, method and vertical profile. *Marine Chemistry*, *48*(2), 151–156. https://doi.org/10.1016/0304-4203(94)00048-I.,

Truesdale, V. W., Watts, S. F., & Rendell, A. R. (2001). On the possibility of iodide oxidation in the near-surface of the Black Sea and its implications to iodine in the general ocean. *Deep Sea Research Part I: Oceanographic Research Papers*, *48*(11), 2397–2412. https://doi.org/10.1016/S0967-0637(01)00021-8

Tsunogai, S., & Sase, T. (1969). Formation of iodide-iodine in the ocean. *Deep-Sea Research and Oceanographic Abstracts*, *16*(5), 489–496. https://doi.org/10.1016/0011-7471(69)90037-0

Wadley, M. R., Stevens, D. P., Jickells, T. D., Hughes, C., Chance, R., Hepach, H., et al. (2020). A global model for iodine speciation in the upper ocean. *Global Biogeochemical Cycles*, *34*(9), e2019GB006467. https://doi.org/10.1029/2019GB006467

Westberry, T., Behrenfeld, M. J., Siegel, D. A., Boss, E., & Boss, E. (2008). Carbon-based primary productivity modeling with vertically resolved photoacclimation. *Global Biogeochemical Cycles*, *22*(2). https://doi.org/10.1029/2007GB003078

Wong, G. T. F., & Cheng, X. H. (2008). Dissolved inorganic and organic iodine in the Chesapeake Bay and adjacent Atlantic waters: Speciation changes through an estuarine system. *Marine Chemistry*, *111*(3–4), 221–232. https://doi.org/10.1016/j.marchem.2008.05.006

Wong, G. T. F., Piumsomboon, A. U., & Dunstan, W. M. (2002). The transformation of iodate to iodide in marine phytoplankton cultures. *Marine Ecology Progress Series*, *237*, 27–39. https://doi.org/10.3354/meps237027

Wong, G. T. F. (2001). Coupling iodine speciation to primary, regenerated or new production: A re-evaluation (Vol. *18*). https://doi.org/10.1016/S0967-0637(00)00097-2

Wong, G. T. F., & Brewer, P. G. (1974). The determination and distribution of iodate in South Atlantic waters. *Journal of Marine Research*, *32*, 25–36.

Wong, G. T. F., Brewer, P. G., & Spencer, D. W. (1976). The distribution of particulate iodine in the Atlantic Ocean. *Earth and Planetary Science Letters*, *32*(2), 441–450. https://doi.org/10.1016/0012-821X(76)90084-4

Wong, G. T. F., Takayanagi, K., & Todd, J. F. (1985). Dissolved iodine in waters overlying and in the orca basin, gulf of Mexico. *Marine Chemistry*, *17*(2), 177–183. https://doi.org/10.1016/0304-4203(85)90072-6

Yeager, C. M., Amachi, S., Grandbois, R., Kaplan, D. I., Xu, C., Schwehr, K. A., & Santschi, P. H. (2017). Microbial transformation of iodine: From radioisotopes to iodine deficiency. *Advances in Applied Microbiology*, *101*, 83–136. Elsevier. https://doi.org/10.1016/bs.aambs.2017.07.002

Zhou, X., Jenkyns, H. C., Lu, W., Hardisty, D. S., Owens, J. D., Lyons, T. W., et al. (2017). Organically bound iodine as a bottom-water redox proxy: Preliminary validation and application. *Chemical Geology*, *457*, 95–106. https://doi.org/10.1016/j.chemgeo.2017.03.016